

# Silylanions: Inversion Barriers and NMR Chemical Shifts

Michaela Flock\* and Christoph Marschner<sup>[a]</sup>

**Abstract:**  $\alpha$ -Substituent effects on inversion barriers and NMR chemical shifts have been studied on a set of silyl anions,  $[\text{X}_{3-n}\text{Y}_n\text{Si}]^-$  (X, Y = H, CH<sub>3</sub>, and SiH<sub>3</sub>). The MP2/6-31 + G\* optimized structures show a pattern of increasing inversion barriers with augmenting numbers of methyl substituents. The highest barrier of 48.5 kcal mol<sup>-1</sup> is ob-

tained for the (CH<sub>3</sub>)<sub>3</sub>Si<sup>-</sup> ion. The silyl group displays the opposite effect by decreasing the inversion barrier to a minimum of 16.3 kcal mol<sup>-1</sup> in (SiH<sub>3</sub>)<sub>3</sub>Si<sup>-</sup>. The influence of counterions

**Keywords:** ab initio calculations • ion pairs • silanes • silyl anions

on these barriers is probed by addition of a lithium or potassium cation. In most cases, a decrease of the energy barriers with respect to the bare anions is observed. The <sup>29</sup>Si NMR chemical shifts calculated at the IGLO-DFT and GIAO-MP2 level of theory are also analyzed in view of the substituents and counterions.

## Introduction

Silyl groups find widespread use as protective groups and for directing purposes in organic<sup>[1]</sup> and inorganic chemistry.<sup>[2–4]</sup> While the incorporation of these groups is accomplished frequently by electrophilic silyl reagents, silyl anions have also recently gained some importance in this respect.<sup>[5, 6]</sup> In the context of controlled formation of polysilanes with defined arrangement of the chain,<sup>[7]</sup> the configurational stability of silyl anion intermediates is of special interest for an optimization of the reaction conditions. The influence of size and nature of the substituents on the configurational stability of the silyl anions is therefore an interesting area of research.

While several bulky alkyl, aryl, and silyl-substituted silyl anions are known, only a rather low number of compounds with other functional groups, such as amino<sup>[8–10]</sup> or alkoxy<sup>[11]</sup> groups, have been synthesized. In solution, silyl anions usually are complexed with, for example, alkali or alkaline-earth metal cations.<sup>[2–6]</sup> X-ray structure analyses show a high affinity of polar solvent molecules, such as tetrahydrofuran (THF), towards the cations. Usually two to three THF molecules interact with the respective cation,<sup>[6, 9, 10, 12, 13]</sup> which was also confirmed by <sup>29</sup>Si NMR experiments<sup>[5, 9, 10, 14]</sup> in the solution and solid state. This kind of interaction in the solid state is even observed with apolar solvents, such as toluene or

benzene, and in solution leads to <sup>29</sup>Si NMR shift differences of up to 10 ppm.<sup>[14–17]</sup> Although X-ray crystallography is a powerful tool for solving the crystal structure of silyl anion complexes, additional <sup>29</sup>Si NMR measurements are often required to understand the reacting species. Especially when solid-state samples are not available, structure assignment is primarily based on <sup>29</sup>Si NMR spectroscopy.<sup>[18]</sup> Furthermore, NMR spectroscopy allows monitoring of reactions and, with the aid of coalescence experiments, an estimate of the inversion barriers is possible.<sup>[19]</sup>

Computational chemistry provides yet another way to gain insight into electronic and structural features of the highly reactive silyl anions. Owing to computational limitations, many of the previous theoretical studies were restricted to the H<sub>3</sub>Si<sup>-</sup> and H<sub>2</sub>XSi<sup>-</sup> ions. For these species, substituent effects on structures, inversion barriers, and electron affinities have been investigated at various levels of theory.<sup>[20–24]</sup> Comparing the respective silyl and carbanions, Hopkinson et al.<sup>[20, 21]</sup> found much higher inversion barriers for the silicon species. In H<sub>2</sub>XSi<sup>-</sup> anions the Si–X distance increases in the series X = CH<sub>3</sub>, NH<sub>2</sub>, OH, and F.<sup>[21]</sup> A similar trend has been observed for carbanions.<sup>[25]</sup> It was stated that electron-withdrawing substituents donating electrons by resonance ( $\pi$  donor) or withdrawing them by induction ( $\sigma$  acceptors) raise the inversion barrier.<sup>[26]</sup>

The H<sub>3</sub>Si anion has been the target of several experimental<sup>[27–30]</sup> and theoretical investigations.<sup>[30–34]</sup> Although the structure of H<sub>3</sub>Si<sup>-</sup> is expected to be similar to that of NH<sub>3</sub>, ab initio calculations show that tricoordinate silicon is distinctly more pyramidal and has larger inversion barriers. The most recent result of 23.9 ± 0.3 kcal mol<sup>-1</sup> for the inversion barrier was obtained by CCSD(T)-R 12 calculations with corrections.<sup>[35]</sup>

[a] Dipl.-Ing. Dr. techn. M. Flock,  
Ao. Univ.-Prof. Dipl.-Ing. Dr. techn. C. Marschner  
Institut für Anorganische Chemie  
Technische Universität Graz  
Stremayrg. 16, 8010 Graz (Austria)  
Fax: (+43) 316-873-8701  
E-mail: flock@anorg.tu-graz.ac.at

Schleyer and Clark<sup>[36]</sup> reported a  $R_3SiM$  complex, namely  $H_3SiLi$ , with an inverted structure (i.e. the cation is attached to R instead of Si) having a 2.4 kcal mol<sup>-1</sup> preference at the MP4/6-31G\*\* level of theory. They argue, however, that the order of stability should be reversed in solution. For the derivative with R=Cl,<sup>[18]</sup> a preference for the inverted structure of 26.0 kcal mol<sup>-1</sup><sup>[37]</sup> was obtained. Detailed density functional theory (DFT) studies on  $X_nH_{3-n}SiM$  (M = Li, Na, X = F, Cl, Br) molecules showed an increased stability of the inverted forms with increasing number and size of the halogens.<sup>[38, 39]</sup>

Not only the silicon substituents, but also the choice of the counterion influence the stability of the silyl anion complexes.<sup>[40–42]</sup> Calculations on  $H_3SiNa$  show a preference for the tetrahedral minimum over the inverted structure (1.55 kcal mol<sup>-1</sup> at the MP4/6-31G\* level<sup>[40]</sup>). In the sodium alcoholate  $H_3Si$  complex, however, the inverted form is more stable, as was proven by X-ray structure analysis and ab initio calculations.<sup>[40]</sup> In the case of  $H_3SiK$ , the tetrahedral conformer has been found to be more stable.<sup>[41, 42]</sup>

Interconversion of inverted and tetrahedral conformers is not only achieved via a planar transition structure (TS) but also via a pyramidal TS with the cation moving along the molecular surface. Both  $R_3SiM$  isomerization mechanisms have so far only been studied for  $H_3SiLi$ .<sup>[36]</sup> In this case, the second mechanism was found to be clearly energetically preferable. For racemization reactions of chiral silyl anions, both mechanisms have to be considered. Especially in solution, dimeric inversion processes are also likely to occur, but are not the target of our present study.

Herein we apply ab initio calculations to investigate the effect of  $\alpha$ -substituents on the inversion barriers and NMR chemical shifts on the bare anions,  $[X_{3-n}Y_nSi]^-$  with X, Y = H, CH<sub>3</sub>, and SiH<sub>3</sub>. The models are then extended by addition of the counterions, Li<sup>+</sup> and K<sup>+</sup>, to study their influence on the configuration stability and trends in the NMR spectroscopic shifts of silyl anions. Solvent effects and  $\beta$ - and  $\gamma$ -substituent effects as well as the effects of other  $\alpha$ -substituents (i.e.  $\pi$ -donors NH<sub>2</sub> and PH<sub>2</sub>) will be treated in a subsequent article.

## Computational Methods

All structures were optimized at the MP2 and for comparison at the DFT/B3LYP<sup>[43a,b,c]</sup> level of theory using the 6-31 + G\* basis sets. The slightly larger 6-31 ++ G\* basis set has been employed for the potassium cation. The nature of the stationary points was verified by analytical calculation of the second derivatives of the energy. Minima have no negative eigenvalues, transition structures have exactly one. Atomic charges  $q$  were obtained by natural bond orbital (NBO) natural population analysis as implemented in the Gaussian 98<sup>[43a,d]</sup> program suite.

The <sup>29</sup>Si shieldings,  $\sigma(^{29}Si)$ , were computed at the some-over-states density functional perturbation theory level (SOS-DFPT) with the deMon<sup>[44–46]</sup> program. The Perdew–Wang<sup>[47]</sup> gradient-corrected exchange-correlation functional was applied together with IGLO-II basis sets.<sup>[48]</sup> Tetramethylsilane (TMS), optimized at the MP2/6-31 + G(d) level of theory, was used as a reference molecule with  $\sigma(^{29}Si) = 349.5$  ppm.

Additionally, GIAO MP2/6-311 + G\* calculations have been performed using Gaussian 98. The nuclear magnetic shielding of TMS at this level of theory amounts to  $\sigma(^{29}Si) = 377.0$  ppm.

Throughout this paper, bond lengths are given in Ångstroms (Å), bond angles in degrees, and relative energies in kcal mol<sup>-1</sup>.

## Results and Discussion

**Geometries:** The substituents used in our study comprise hydrogen, methyl and silyl groups. The Pauling electronegativities of the selected  $\alpha$ -substituents vary from 1.90 for silicon, and 2.20 for hydrogen, to 2.55 for carbon. Hence, in the context of  $[X_{3-n}Y_nSi]^-$ , the methyl group acts not as a  $\sigma$  donor, as often found in organic chemistry, but as a  $\sigma$  acceptor. Lithium and potassium are with 0.98 and 0.82 more electro-positive than silicon.

Therefore, the most pronounced substituent effect in this set can be expected for the methyl group withdrawing electrons from the silicon center. The silyl group, on the contrary, should, as known from the respective carbanions,<sup>[49, 50]</sup> rather stabilize the negative charge on the central silicon.

Table 1 lists bond lengths and, as a measure of the pyramidal nature, bond angle sums for our set of  $[X_{3-n}Y_nSi]^-$  ions with X, Y = H, CH<sub>3</sub>, and SiH<sub>3</sub>. Only the bond distances in the series X–SiY<sub>2</sub> with X = H and SiH<sub>3</sub> follow the electronegativity order of the  $\alpha$ -substituents. Natural bond orbital analysis (NBO) reveals hyperconjugative effects stemming from electron donation of the lone pair electrons on the central Si into  $\sigma^*$  orbitals of substituent C–H and Si–H bonds, causing these bonds to be slightly elongated. The transition structures involved for inversion are planar and have about 0.05 Å shorter Si–X and Si–Y bond lengths than the respective minima. For  $[(CH_3)_3Si]^-$  an additional, energetically less favorable T-shaped transition structure could be located.

Table 1. Bond lengths [Å] and bond angle sums ( $\Sigma\alpha$ ) of  $[XY_2Si]^-$  (X, Y = H, CH<sub>3</sub>, and SiH<sub>3</sub>) ions calculated at the MP2/6-31 + G\* level.

X		$[H_2XSi]^-$	$[(CH_3)_2XSi]^-$	$[(SiH_3)_2XSi]^-$
H	Si–X	1.538	1.547	1.531
	Si–Y	1.538	1.964	2.358
	$\Sigma\alpha$	289.3	292.2	286.2
CH <sub>3</sub>	Si–X	1.973	1.954	1.970
	Si–Y	1.542	1.954	2.358
	$\Sigma\alpha$	292.0	292.9	290.5
SiH <sub>3</sub>	Si–X	2.369	2.375	2.352
	Si–Y	1.533	1.962	2.352
	$\Sigma\alpha$	287.0	291.2	284.7

In sharp contrast to the  $\alpha$ -silyl-substituted carbanions, which are almost planar,<sup>[51, 52]</sup> none of our silyl anion minima exhibits planar or even near planar geometry. The bond angle sums range from 284.7–292.9°. While the tris(silyl)silyl anion,  $[(SiH_3)_3Si]^-$ , exhibits the most pyramidal structure, a bond angle sum of 358.1° is found for the homologous tris(silyl)-carbanion,  $[(SiH_3)_3C]^-$ . With 0.88 kcal mol<sup>-1</sup> at MP2/6-31 + G\*,<sup>[53]</sup> the inversion barrier of  $[(SiH_3)_3C]^-$  is quite small. In the presence of a lithium cation, we find that both the pyramidal nature and the inversion barrier of  $[(SiH_3)_3C]^-$  increase (the bond angle sum equals 340.2,  $E_{inv} = 1.92$  kcal mol<sup>-1</sup>).

Table 2 lists the population of the lone pair and the charges on the silicon atom obtained by NBO, analyses. The silicon charges nicely mirror the electronegativity ordering of the substituents. While Si bears a charge of +0.67 in  $[(CH_3)_3Si]^-$ ,

Table 2. Inversion barriers,  $E_{\text{inv}}$  (including zero-point energy) in kcal mol<sup>-1</sup> and silicon NPA charge, and Si lone pair occupation (LP) of the  $[X_{3-n}Y_n\text{Si}]^-$  ions (X, Y = H, CH<sub>3</sub>, SiH<sub>3</sub>) calculated at the MP2/6-31 + G\* level. The  $\delta(^{29}\text{Si})$  chemical shifts were obtained by IGLO-DFT and GIAO-MP2 calculations. The shielding of the reference molecule tetramethylsilane (TMS) is  $\sigma(^{29}\text{Si}) = 349.5$  and  $\sigma(^{29}\text{Si}) = 377.0$ , respectively.

Anion	$E_{\text{inv}}$ (MP2)	$E_{\text{inv}}$ (DFT)	$q(\text{Si})$	LP	$\delta(\text{Si})$ (MP2)	$\delta(\text{Si})$ (DFT)
$[\text{H}_3\text{Si}]^-$	26.0	26.3	-0.27	2.00	-216.6	-193.5
$[\text{H}_2(\text{CH}_3)\text{Si}]^-$	30.0	30.0	0.14	1.99	-102.1	-111.5
$[\text{H}_2(\text{SiH}_3)\text{Si}]^-$	22.7	23.5	-0.24	1.96	-204.9	-214.0
$[\text{H}(\text{CH}_3)_2\text{Si}]^-$	36.3	36.1	0.43	1.97	-23.6	-62.3
$[\text{H}(\text{SiH}_3)_2\text{Si}]^-$	19.3	20.6	-0.38	1.92	-225.6	-237.8
$[(\text{CH}_3)_3\text{Si}]^-$	48.7	47.3	0.67	1.95	-10.5	-58.4
$[(\text{CH}_3)_2(\text{SiH}_3)\text{Si}]^-$	29.8	29.3	0.29	1.94	-56.1	-92.1
$[\text{CH}_3(\text{SiH}_3)_2\text{Si}]^-$	20.9	21.2	-0.13	1.91	-146.6	-169.1
$[(\text{SiH}_3)_3\text{Si}]^-$	16.7	17.5	-0.59	1.89	-262.4	-265.4

the negative charge (-0.59) of the anionic silicon is stabilized by the silyl substituents in the tris(silyl)silyl anion.

Previous theoretical comparison of  $[\text{H}_2\text{XSi}]^-$  anions<sup>[20, 24, 54, 55]</sup> with the respective hydrosilanes showed that deprotonation causes the Si-X bond lengths to increase, while the bond angles decrease in a similar fashion to the carbanions.<sup>[25]</sup> Consequently, we expect that the addition of a counterion forming a tetrahedral structure provokes a decrease of the Si-X, Y bond lengths. Furthermore, tetrahedral structures with the negative charge mainly located at the central Si atom should have shorter Si-M (M = Li, K) distances than those with the negative charge distributed mainly on the substituents.

Indeed we find that all Si-X, Y bonds shorten by 0.012–0.055 Å in the lithiated silanes. In addition, the Li-Si distance is shortest in  $(\text{SiH}_3)_3\text{SiLi}$  (2.482 Å) and longest in  $(\text{CH}_3)_3\text{SiLi}$  (2.540 Å). The X-ray structures of  $(\text{Me}_3\text{Si})_3\text{SiLi} \cdot 3 \text{ THF}$ , Li-Si 2.6691 Å, and  $\text{Ph}_3\text{SiLi} \cdot 3 \text{ THF}$ , Li-Si 2.6729 Å,<sup>[12]</sup> show a similar trend, but are not directly comparable due to the considerably larger substituents and the coordinated THF molecules. Crystal packing effects are also likely to additionally influence the bond lengths (Table 3).

The larger potassium counterion has a weaker effect than lithium. It causes a decrease of Si-X bonds by up to only 0.041 Å. As in the set of lithium complexes, the K-Si distance is shortest in the  $(\text{SiH}_3)_3\text{SiK}$  molecule. In the methyl-substituted silyl anions the K-Si distances are all rather long (Table 4).

In the inverted structures, the cation is mainly stabilized by interactions with the  $\alpha$ -substituent hydrogens or those of the

substituent groups. Both the  $\alpha$ -substituent hydrogen (-0.26 to -0.33) and the hydrogens of the SiH<sub>3</sub> groups (-0.23 to -0.26) bear negative partial charges as obtained by natural population analyses. This is in contrast to the hydrogens of the CH<sub>3</sub> groups, which possess a positive partial charge (0.19 to 0.21).

The inverted lithium and potassium silanes have longer Si-X and Si-Y bond lengths than the bare anions and the tetrahedral structures. In  $\text{H}_2(\text{SiH}_3)\text{SiLi}$  and those molecules with at least two silyl substituents, the Li-Si distances (and in  $\text{H}_3\text{SiK}$  and  $\text{H}_2(\text{CH}_3)\text{SiK}$  the K-Si distances) are longer than in the tetrahedral structures. Most of the inverted structures possess less pyramidal SiR<sub>3</sub> moieties than the tetrahedral conformers.

**Energies:** The stability against inversion is of special interest in the case of chiral silyl anions. The question of which substituents will increase or lower the silicon inversion barriers,  $E_{\text{inv}}$ , then arises. In case of bare silyl anions, only one possibility exists to invert, namely via a planar transition structure. Table 2 lists all  $E_{\text{inv}}$  values and the occupation of the lone pair (LP) for the bare silyl anions. The more SiH<sub>3</sub> groups that bind to the silicon, the lower the inversion barrier. Methyl substituents have an opposite effect. Hence, stepwise exchange of the silyl groups in  $[(\text{SiH}_3)_3\text{Si}]^-$  by methyl groups increases the inversion barrier from 16.7, 20.9, and 29.8 kcal mol<sup>-1</sup> to 48.7 kcal mol<sup>-1</sup> in  $[(\text{CH}_3)_3\text{Si}]^-$ , the highest barrier in our molecule set. Simultaneously, we find that the more silyl substituents there are, the lower the LP occupation numbers (1.89 in  $[(\text{SiH}_3)_3\text{Si}]^-$  versus 1.95 in  $[(\text{CH}_3)_3\text{Si}]^-$ ). NBO

Table 3. Bond lengths [Å] and bond angle sums ( $\Sigma\alpha$ ) of the tetrahedral and the inverted like  $[\text{XY}_2\text{Si}]\text{Li}$  (X, Y = H, CH<sub>3</sub>, SiH<sub>3</sub>) molecules calculated at the MP2/6-31 + G\* level.

X		Tetrahedral			Inverted		
		$\text{H}_2\text{XSiLi}$	$\text{Me}_2\text{XSiLi}$	$(\text{SiH}_3)_2\text{XSiLi}$	$\text{H}_2\text{XSiLi}$	$\text{Me}_2\text{XSiLi}$	$(\text{SiH}_3)_2\text{XSiLi}$
H	Si-X	1.503	1.510	1.504	1.571	1.583	1.558
	Si-Y	1.503	1.919	2.342	1.571	1.995	2.374
	Si-Li	2.497	2.527	2.489	2.377	2.360	2.646
	$\Sigma\alpha$	309.3	311.7	311.7	265.5	283.3	278.7
CH <sub>3</sub>	Si-X	1.921	1.917	1.931	2.006	1.992	1.987
	Si-Y	1.507	1.917	2.344	1.577	1.992	2.362
	Si-Li	2.513	2.540	2.500	2.363	2.334	2.613
	$\Sigma\alpha$	311.2	311.7	313.6	275.2	294.5	295.4
SiH <sub>3</sub>	Si-X	2.344	2.351	2.340	2.400	2.387	2.350
	Si-Y	1.503	1.923	2.340	1.566	1.990	2.350
	Si-Li	2.495	2.521	2.482	2.498	2.457	2.809
	$\Sigma\alpha$	309.9	312.7	312.4	269.1	294.6	292.8

Table 4. Bond lengths [ $\text{\AA}$ ] and bond angle sums ( $\Sigma\alpha$ ) of the tetrahedral and the inverted  $[\text{XY}_2\text{SiK}]$  (X, Y = H,  $\text{CH}_3$ ,  $\text{SiH}_3$ ) molecules calculated at the MP2/6–31 + G\* level.

X		Tetrahedral			Inverted		
		$\text{H}_2\text{XSiK}$	$\text{Me}_2\text{XSiK}$	$(\text{SiH}_3)_2\text{XSiK}$	$\text{H}_2\text{XSiK}$	$\text{Me}_2\text{XSiK}$	$(\text{SiH}_3)_2\text{XSiK}$
H	Si–X	1.510	1.518	1.510	1.560	1.572	1.546
	Si–Y	1.510	1.929	2.342	1.560	1.979	2.365
	Si–K	3.229	3.313	3.266	3.200	3.370	3.511
	$\Sigma\alpha$	303.4	306.6	304.5	276.0	291.7	290.9
$\text{CH}_3$	Si–X	1.933	1.924	1.937	1.985	1.995	1.968
	Si–Y	1.514	1.924	2.344	1.568	1.995	2.349
	Si–K	3.290	3.335	3.282	3.260	3.476	3.735
	$\Sigma\alpha$	305.6	307.1	308.9	284.5	297.2	312.1
$\text{SiH}_3$	Si–X	2.346	2.354	2.338	2.384	2.375	2.339
	Si–Y	1.510	1.931	2.338	1.555	1.967	2.339
	Si–K	3.269	3.309	3.263	3.318	3.610	3.867
	$\Sigma\alpha$	302.8	308.2	307.1	279.8	311.4	309.9

analyses show that the interaction between the LP and the  $\sigma^*$  Si–H antibonding orbitals of the silyl substituents is stronger than with the  $\sigma^*$  C–H. In the course of inversion, more energy is therefore needed to redistribute the lone pair electrons in the presence of methyl substituents.

In the neutral ion complexes, the inverted structures sometimes are more stable than the tetrahedral structures. This reversed stability has been reported for  $\text{H}_3\text{SiLi}$ <sup>[36]</sup> and for halogenated silyllithium and -sodium compounds<sup>[37–39]</sup> in the gas phase. In the solid state or in solution, small energetic stabilities might be reversed as for  $\text{H}_3\text{SiNa}$ .<sup>[40]</sup> The inverted structure was observed in solid and liquid phase spectroscopic studies, while gas phase calculations of the isolated molecule yield the tetrahedral minimum as being more stable.

As listed in Table 5, we find four lithium ion pairs,  $\text{H}_3\text{SiLi}$  ( $E_{\text{rel}} = 0.31 \text{ kcal mol}^{-1}$ ),  $\text{H}_2(\text{SiH}_3)\text{SiLi}$  ( $E_{\text{rel}} = 0.36 \text{ kcal mol}^{-1}$ ),  $\text{H}(\text{SiH}_3)_2\text{SiLi}$  ( $E_{\text{rel}} = 2.48 \text{ kcal mol}^{-1}$ ) and  $(\text{SiH}_3)_3\text{SiLi}$  ( $E_{\text{rel}} = 6.22 \text{ kcal mol}^{-1}$ ) with an inverted structure. Evidently, the presence of methyl groups stabilizes the tetrahedral structures. This stabilization can be rationalized by the unfavorable interaction of the cation with the methyl hydrogens in the inverted structures, as their partial charges are positive. Consequently the electrostatic interaction with the cation is repulsive and causes destabilization. The silyl group with negative hydrogen charges, on the other hand, yields favorable electrostatic interactions.

The potassium compounds present a similar picture (Table 6). In contrast to the lithium analogue,  $(\text{SiH}_3)_3\text{SiK}$  is more stable in its tetrahedral form ( $\Delta E = 1.65 \text{ kcal mol}^{-1}$ ). In

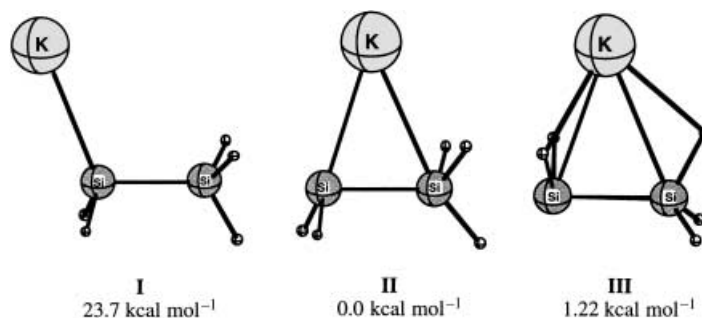
Table 5. Absolute energies in hartree and inversion barriers [ $\text{kcal mol}^{-1}$ ] of the tetrahedral (1) and the inverted structures (2) of the  $[\text{X}_{3-n}\text{Y}_n\text{SiLi}]$  (X, Y = H,  $\text{CH}_3$ ,  $\text{SiH}_3$ ) molecules obtained at the MP2/6–31 + G\*. Relative energies calculated at the B3LYP/6–31 + G\* level are given in parenthesis.

Molecule	$E_1$	$E_2$	$\Delta E_{(\text{ITS})}$	$\Delta E_{(\text{ZTS})}$
$\text{H}_3\text{SiLi}$	–298.17346	–298.17395	25.9 (25.2)	26.2 (26.5)
$(\text{CH}_3)_3\text{SiLi}$	–415.70364	–415.68369	52.8 (50.0)	40.2 (40.2)
$(\text{SiH}_3)_3\text{SiLi}$	–1168.68364	–1168.69355	9.2 (9.8)	15.4 (15.8)
$\text{H}_2\text{CH}_3\text{SiLi}$	–337.34791	–337.34036	30.7 (29.8)	25.9 (26.2)
$\text{H}_2\text{SiH}_3\text{SiLi}$	–588.34087	–588.34144	19.8 (18.2)	20.3 (20.9)
$\text{H}(\text{CH}_3)_2\text{SiLi}$	–376.52451	–376.51110	37.5 (36.2)	29.0 (29.3)
$\text{H}(\text{SiH}_3)_2\text{SiLi}$	–878.51073	–878.51469	15.3 (15.6)	17.8 (18.4)
$(\text{CH}_3)_2\text{SiH}_3\text{SiLi}$	–666.69174	–666.68031	29.4 (28.1)	22.2 (22.3)
$\text{CH}_3(\text{SiH}_3)_2\text{SiLi}$	–917.68514	–917.68372	14.3 (14.1)	13.4 (13.5)

Table 6. Energies of the tetrahedral (1) and the inverted structures (2) in hartree and inversion barriers ( $\text{kcal mol}^{-1}$ ) for the  $[\text{X}_{3-n}\text{Y}_n\text{SiK}]$  (X, Y = H,  $\text{CH}_3$ ,  $\text{SiH}_3$ ) molecules obtained by MP2/6–31 + G\* calculations. Relative energies calculated at the B3LYP/6–31 + G\* level are given in parenthesis.

Molecule	$E_1$	$E_2$	$\Delta E_{(\text{ITS})}$	$\Delta E_{(\text{ZTS})}$
$\text{H}_3\text{SiK}$	–889.84140	–889.83939	24.4 (22.2)	23.1 (21.4)
$(\text{CH}_3)_3\text{SiK}$	–1007.36964	–1007.33511	49.6 (43.3)	27.9 (24.4)
$(\text{SiH}_3)_3\text{SiK}$	–1760.35945	–1760.35682	13.5 (13.3)	11.8 (12.7)
$\text{H}_2\text{CH}_3\text{SiK}$	–929.01472	–929.00155	28.3 (25.9)	20.1 (19.3)
$\text{H}_2\text{SiH}_3\text{SiK}$	–1180.04997	–1180.04803	20.0 (19.5)	18.8 (17.8)
$\text{H}(\text{CH}_3)_2\text{SiK}$	–968.19061	–968.17164	33.5 (31.3)	21.6 (19.2)
$\text{H}(\text{SiH}_3)_2\text{SiK}$	–1470.18459	–1470.22094	7.6 (16.8)	15.2 (15.0)
$(\text{CH}_3)_2\text{SiH}_3\text{SiK}$	–1258.36086	–1258.33890	29.8 (27.7)	16.0 (15.1)
$\text{CH}_3(\text{SiH}_3)_2\text{SiK}$	–1509.35771	–1509.34591	19.7 (19.2)	12.3 (12.6)

$(\text{SiH}_3)_2\text{H}_2\text{SiK}$  and  $(\text{SiH}_3)_2\text{HSiK}$  the cation gains additional stability by interaction with one of the silyl groups forming slightly distorted but energetically favorable pseudo-tetrahedral structures (Figure 1). This structure is only stable in the

Figure 1. The tetrahedral (I), distorted (II), and inverted (III) minimum structures of  $(\text{SiH}_3)_2\text{H}_2\text{SiK}$  calculated at the MP2/6–31 + G\* level.

gas phase. In preliminary calculations at the BLYP/6-31G level, we surrounded the potassium ion in  $\text{H}_2(\text{SiH}_3)\text{SiK}$  by three dimethyl ether molecules to model the effect of tetrahydrofuran. During the geometry optimization, the distorted structure vanishes and the tetrahedral geometry becomes the most stable conformer. Generally the MP2 and DFT/B3LYP calculated structures and energies are quite similar.

The addition of a counterion gives rise to two possible pathways connecting the tetrahedral and the inverted struc-

tures. The first, **RP1**, proceeds via a planar transition structure. The second, **RP2**, is more complex, having transition structures with a pyramidal silyl moiety. This pathway can be described as the cation moving over the silyl anion's surface. In the case of a racemisation reaction, both pathways are involved.

In the case of  $\text{H}_3\text{SiLi}$ , **RP2** was demonstrated to have a much lower barrier than the inversion via the planar transition structure, **RP1**, (13.9 versus  $24.5 \text{ kcal mol}^{-1}$  at MP4/6-31G\*\*).<sup>[36]</sup> This is not necessarily true for all the other ion pairs in the gas phase.

$(\text{SiH}_3)_3\text{SiLi}$ , for instance, has a preference for the umbrella-like structure (Figure 2). On **RP1** the barrier to the tetrahedral geometry is  $15.4 \text{ kcal mol}^{-1}$ , while on **RP2**  $18.2 \text{ kcal mol}^{-1}$  are necessary. For the reversed reaction,  $9.15$  (**RP1**) or  $11.9 \text{ kcal mol}^{-1}$  (**RP2**) as the highest barrier is needed.

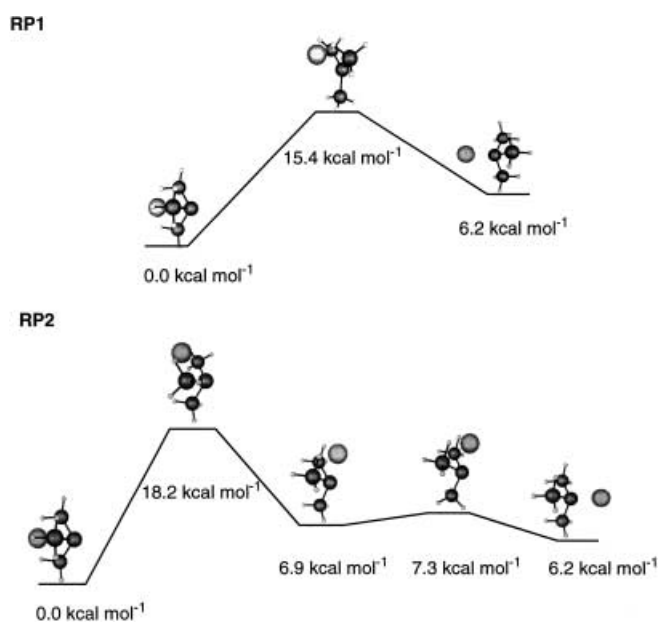


Figure 2. The inversion of  $(\text{SiH}_3)_3\text{SiLi}$ . **RP1** depicts the direct inversion via a planar transition structure, and **RP2** the inversion through cation movement along the silyl moiety.

For the racemization of a chiral silyl anion in the gas phase, however, both isomerization reactions are required, as depicted in Figure 3 using the chiral  $(\text{SiH}_3)(\text{CH}_3)\text{HSiLi}$  molecule.

The conventional  $(\text{SiH}_3)(\text{CH}_3)\text{HSiLi}$  geometry is  $3.66 \text{ kcal mol}^{-1}$  more stable than the inverted conformer. Consequently, the first reaction (either inversion (**RP1**) or counterion movement (**RP2**)) yields the inverted umbrella-like minimum structure. Starting with **RP1**, the energy barrier to the umbrella-like structure is  $23.1 \text{ kcal mol}^{-1}$ . To form the enantiomer of the initial structure the cation has to move along **RP2** with a barrier of  $8.11 \text{ kcal mol}^{-1}$ . Or, starting the racemization with **RP2**, a barrier of  $11.8 \text{ kcal mol}^{-1}$  has to be surmounted to reach the umbrella-like structure and then **RP1** with an inversion barrier of  $19.4 \text{ kcal mol}^{-1}$ .

For our molecule set, we calculated the inversion barriers belonging to **RP1**. In dependence of the  $\alpha$ -substituent and

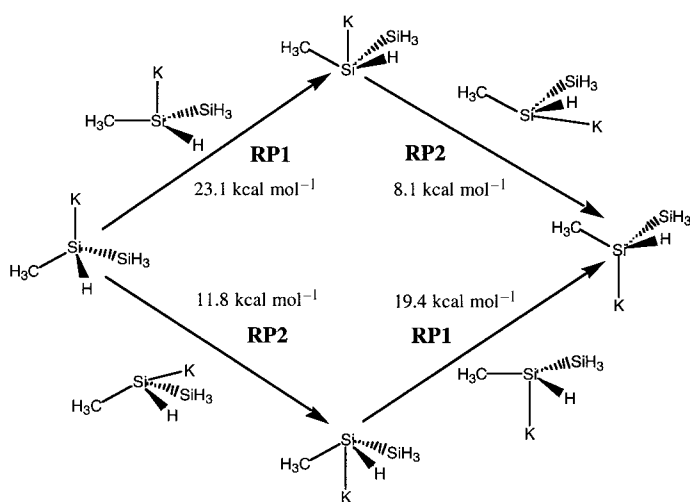


Figure 3. Scheme of the full racemization process for  $(\text{SiH}_3)(\text{CH}_3)\text{HSiLi}$ . **RP1** proceeds via an approximately planar transition structure, while the silyl moiety of the transition structure in **RP2** is still pyramidal.

counterion, some trends become apparent for the barrier heights.

Lithium complexes of  $[\text{X}_{3-n}\text{Y}_n\text{Si}]^-$  with X, Y = H,  $\text{CH}_3$  are more stable than those of the bare anions and of the respective potassium complexes. Potassium as counterion produces fewer changes in stabilization as compared to the bare ions. The difference amounts only to  $+1.1$  to  $-3.4 \text{ kcal mol}^{-1}$ . In general, potassium has a stronger stabilizing effect on all but  $[\text{H}_n(\text{CH}_3)_{3-n}\text{Si}]^-$  ions. For the alkyl-substituted silyl anions, lithium as the counterion provides better configurational stability than potassium.

**Chemical shifts:** One of the most effective methods to monitor the formation and reaction of silyl anions is  $^{29}\text{Si}$  NMR spectroscopy. For silanes, an empirical correlation between chemical shift and ligand electronegativity sum or the charge of the silicon atom has been proposed several times. The  $^{29}\text{Si}$  NMR correlation curve is usually a paraboloid<sup>[56]</sup> with the turning point formed by molecules with highly electronegative  $\alpha$ -substituents, such as oxygen, nitrogen, or halides.  $^{29}\text{Si}$  NMR measurements are mostly performed in the solid state or solution. The solvent molecules, often THF or toluene, rather bind to the cation<sup>[12]</sup> and cause  $^{29}\text{Si}$  shift differences in the range of  $\pm 10 \text{ ppm}$ .<sup>[5]</sup> A similar influence is observed for the chosen counterion.

A recent work of Heine et al.<sup>[57]</sup> shows that DFT calculations of the  $^{29}\text{Si}$  NMR chemical shifts of silanes yield rather poor results as compared to MP2. We use both types of calculations to evaluate if this also applies to the silyl anions.

The calculated  $^{29}\text{Si}$  NMR chemical shifts of our bare silyl anion set span a range from  $-58.4$  to  $-265.4 \text{ ppm}$  at the DFT and  $-10.5$  to  $-262.4 \text{ ppm}$  at the MP2 level. The most shielded is the silyl anion with the highest electron density around the silicon, which is  $[(\text{SiH}_3)_3\text{Si}]^-$  according to the NPA charges. Stepwise substitution of silyl by methyl groups reduces the electron density around the silicon center. Associated is a stepwise increase of the  $^{29}\text{Si}$  chemical shift, as can be gathered from Table 2. This substitution effect on

$\delta(^{29}\text{Si})$  is not linear, but instead shows a sagging behavior, as previously reported for silanes.<sup>[56, 58]</sup>

The difference between DFT and MP2 values is only significant for the molecules containing methyl substituents. In these cases the GIAO-MP2 method yields lower field shifts, such as for  $[(\text{CH}_3)_3\text{Si}]^-$  –10.5 ppm compared to –58.4 ppm with IGLO-DFT methods. Bearing in mind that the measured value for  $[(\text{CH}_3)_3\text{Si}]\text{Li}$  is –32.8 ppm,<sup>[14]</sup> it seems plausible to expect the free anion's chemical shift at a higher field.

Inclusion of the counterions to form tetrahedral geometries reduces the partial charge on the silicon nucleus, causing  $\delta(^{29}\text{Si})$  to shift to a lower field (see Table 7 and Table 8). At the DFT level of theory, the lithiated silanes resonate, with the exception of  $\text{H}(\text{CH}_3)_2\text{SiLi}$ , at up to a 20 ppm higher field than the respective potassium compounds. GIAO-MP2 yields additional exceptions for  $[\text{H}(\text{CH}_3)_2\text{Si}]\text{Li}$ ,  $[(\text{SiH}_3)_2(\text{CH}_3)\text{Si}]\text{Li}$ , and  $[(\text{SiH}_3)(\text{CH}_3)_2\text{Si}]\text{Li}$ .

Table 7. Silicon charge as obtained from NPA analyses, and  $^{29}\text{Si}$  NMR chemical shifts for the tetrahedral  $[\text{X}_{3-n}\text{Y}_n\text{Si}]\text{Li}$  (X, Y = H,  $\text{CH}_3$ ,  $\text{SiH}_3$ ) molecules calculated at the GIAO-MP2 and IGLO-DFT level of theory. The chemical shifts of the respective inverted minimum structures are given in parentheses. Experimentally determined data refer to compounds with  $\text{Me}_3\text{Si}$  groups instead of  $\text{H}_3\text{Si}$ .

Molecule	$q(\text{Si})$	$\delta(\text{Si})$ (MP2)	$\delta(\text{Si})$ (DFT)	$\delta(\text{Si})$ exp.
$\text{H}_3\text{SiLi}$	–0.10	–172.7	–176.2 (–226.0)	–
$(\text{CH}_3)_3\text{SiLi}$	0.84	–12.5	–31.3 (–100.9)	–32.8 <sup>[14]</sup>
$(\text{SiH}_3)_3\text{SiLi}$	–0.86	–219.8	–227.9 (–297.1)	–185.4 <sup>[60]</sup>
$\text{H}_2\text{CH}_3\text{SiLi}$	0.23	–107.2	–115.4 (–135.6)	–
$\text{H}_2\text{SiH}_3\text{SiLi}$	–0.32	–179.4	–189.1 (–205.0)	–
$\text{H}(\text{CH}_3)_2\text{SiLi}$	0.54	–51.7	–66.4 (–86.6)	–71.8 <sup>[59]</sup>
$\text{H}(\text{SiH}_3)_2\text{SiLi}$	–0.57	–194.5	–206.0 (–235.5)	–
$(\text{CH}_3)_2\text{SiH}_3\text{SiLi}$	0.31	–56.8	–76.0 (–148.2)	–74.9 <sup>[14]</sup>
$\text{CH}_3(\text{SiH}_3)_2\text{SiLi}$	–0.26	–128.5	–144.2 (–216.2)	–133.8 <sup>[14]</sup>

Table 8. Silicon charge as obtained from NPA analyses, and  $^{29}\text{Si}$  NMR chemical shifts for the tetrahedral  $[\text{X}_{3-n}\text{Y}_n\text{Si}]\text{K}$  (X, Y = H,  $\text{CH}_3$ ,  $\text{SiH}_3$ ) molecules calculated at the GIAO-MP2 and IGLO-DFT level of theory. The chemical shifts of the respective inverted minimum structures are given in parentheses. Experimentally determined data refer to compounds with  $\text{Me}_3\text{Si}$  groups instead of  $\text{H}_3\text{Si}$ .

Molecule	$q(\text{Si})$	$\delta(\text{Si})$ (MP2)	$\delta(\text{Si})$ (DFT)	$\delta(\text{Si})$ exp.
$\text{H}_3\text{SiK}$	–0.15	–188.4	–165.2 (–248.7)	–165.0 <sup>[56]</sup>
$(\text{CH}_3)_3\text{SiK}$	0.81	1.60	–11.4 (–60.6)	–34.4 <sup>[61]</sup>
$(\text{SiH}_3)_3\text{SiK}$	–0.82	–225.5	–221.5 (–248.1)	–197.6 <sup>[5]</sup>
$\text{H}_2\text{CH}_3\text{SiK}$	0.18	–108.0	–109.3 (–124.3)	–
$\text{H}_2\text{SiH}_3\text{SiK}$	–0.33	190.4	–191.1 (–211.3)	–
$\text{H}(\text{CH}_3)_2\text{SiK}$	0.50	–42.0	–50.6 (58.7)	–
$\text{H}(\text{SiH}_3)_2\text{SiK}$	–0.56	–203.3	–203.8 (–206.2)	–181.1 <sup>[5]</sup>
$(\text{CH}_3)_2\text{SiH}_3\text{SiK}$	0.38	–45.8	–56.2 (–85.3)	–62.9 <sup>[5]</sup>
$\text{CH}_3(\text{SiH}_3)_2\text{SiK}$	–0.24	–125.8	–130.3 (–159.3)	–128.7 <sup>[53]</sup>

Comparison with measured  $^{29}\text{Si}$  chemical shifts is rather difficult, as most of the synthesized silyl anions have larger substituents, such as aryl groups instead of methyl or  $(\text{SiMe}_3)$  groups instead of  $\text{SiH}_3$ . The available experimental  $^{29}\text{Si}$  chemical shifts of the lithium and the potassium complexes are collected in Tables 7 and 8 and compared to the calculated data. The agreement is satisfactory, taking into account the simpler substituents of the model systems and the neglect of

solvent molecules. However, most DFT results are closer to the experiment than the MP2 shifts, which might be due to favorable error cancellations.

Regardless of the method chosen, the calculated chemical shift of  $(\text{CH}_3)_3\text{SiK}$  is always found to be lower than that of  $(\text{CH}_3)_3\text{SiLi}$ . While the agreement between DFT calculated and measured chemical shift is very good for  $(\text{CH}_3)_3\text{SiLi}$ , the calculated value for  $(\text{CH}_3)_3\text{SiK}$  is approximately 20 ppm too high.

The  $\delta(^{29}\text{Si})$  values for the inverted structures calculated with DFT are given in parenthesis in Tables 7 and 8. Since in these structures the cation interacts mostly with the substituents, the chemical shifts are at a higher field compared to the bare anions. Two peculiarities, namely the strong high-field shift of  $(\text{SiH}_3)_3\text{SiLi}$  and the extreme low-field shift of  $\text{H}(\text{CH}_3)_2\text{SiK}$ , should be mentioned. In the case of  $(\text{SiH}_3)_3\text{SiLi}$ , the lithium cation increases the electron density on the silicon nucleus in a way that  $\delta(^{29}\text{Si}) = -297.1$ , 32 ppm lower than for the respective free anion. The calculation with GIAO-MP2 confirms this result, yielding  $\delta(^{29}\text{Si}) = -310.0$ . The other unexpected value, namely  $\delta = 58.7$ , is obtained for the inverted  $\text{H}(\text{CH}_3)_2\text{SiK}$  with IGLO-DFT, caused by an erroneously small HOMO-LUMO gap in the DFT calculation. The respective GIAO-MP2 chemical shift is  $\delta = -31.8$ .

The electronegativity of the substituents is often correlated with the chemical shift with differing significance.<sup>[58]</sup> We find that the linear relationships between the substituent electronegativity sum,  $\Sigma(\text{EN})$ , and  $\delta(^{29}\text{Si})$  (correlation coefficient square,  $cc = 0.71$ ) as well as between the inversion barrier and  $\delta(^{29}\text{Si})$  ( $cc = 0.72$ ) are not high enough to provide a precise predictive tool. The correlation between silicon charge and  $\delta(^{29}\text{Si})$  is somewhat better ( $cc = 0.89$ ), but still not sufficient for firm predictions.

## Conclusion

Silyl substituents, known to stabilize the negative charge and the thermodynamic stability of carbanions, lower the conformational stability of silyl anions, while alkyl groups have the opposite effect. Exchange of silyl substituents against, for instance, methyl increases the inversion barrier from 16.7 (for  $[(\text{SiH}_3)_3\text{Si}]^-$ ) to 48.7 kcal mol<sup>–1</sup> (for  $[(\text{CH}_3)_3\text{Si}]^-$ ). The silyl anions are pyramidal in contrast to the almost planar silyl-substituted carbanions. Addition of a lithium or potassium cation has no drastic influence on the inversion energies.

The tetrahedral structure is the lower energy minimum in all investigated species with at least one methyl substituent. Owing to the favorable electrostatic interactions of the cation with the hydrogens of the silyl groups, some of the inverted silyl-substituted structures are more stable than the tetrahedral conformer.

A relationship between inversion barrier, or the NBO calculated Si charge, and  $^{29}\text{Si}$  NMR chemical shifts could not be established to an accuracy allowing reliable predictions. Comparison with the measured NMR chemical shift data is quite good for the IGLO-DFT calculations, while larger differences are found for the GIAO-MP2 results. To improve the comparison with the experimental values, larger  $\beta$ -

substituents and explicit inclusion of solvent molecules are necessary.

### Acknowledgement

The authors thank Prof. D. R. Salahub, V. Malkin, and O. Malkina for a copy of deMon and the MASTER-NMR program. The Austrian Science Foundation (FWF) is gratefully acknowledged for financial support in the form of a START fellowship (Project Y-120) to C.M.

- [1] E. W. Colvin, *Silicon in Organic Chemistry*, Butterworths, London, **1981**.
- [2] P. D. Lickiss, C. M. Smith, *Coord. Chem. Rev.* **1995**, *145*, 75.
- [3] K. Tamao, A. Kawachi, *Adv. Organomet. Chem.* **1995**, *38*, 1.
- [4] J. Belzner, U. Dehnert, *The Chemistry of Silicon Compounds*, Vol. 2 (Eds.: Z. Rappoport, Y. Apeloig), Wiley, New York, **1998**, p. 780.
- [5] C. Marschner, *Eur. J. Inorg. Chem.* **1998**, *2*, 221.
- [6] Y. Apeloig, M. Yuzefovich, M. Bendikov, D. Bravo-Zhivotovskii, K. Klinkhammer, *Organometallics* **1997**, *16*, 1265.
- [7] E. Fossum, K. Matyjaszewski, *Macromolecules* **1995**, *28*, 1618.
- [8] K. Tamao, A. Kawachi, Y. Ito, *J. Am. Chem. Soc.* **1992**, *114*, 3989.
- [9] A. Kawachi, K. Tamao, *J. Am. Chem. Soc.* **2000**, *122*, 1919.
- [10] C. Strohmann, O. Ulbrich, D. Auer, *Eur. J. Inorg. Chem.* **2001**, 1013.
- [11] K. Tamao, A. Kawachi, *Angew. Chem.* **1995**, *107*, 886; *Angew. Chem. Int. Ed. Engl.* **1995**, 818.
- [12] H. V. R. Dias, M. M. Olmsted, K. Ruhlandt-Senge, P. P. Power, *J. Organomet. Chem.* **1993**, *462*, 1.
- [13] J. D. Farwell, M. F. Lappert, C. Marschner, C. Strissel, T. D. Tilley, *J. Organomet. Chem.* **2000**, *603*, 185.
- [14] M. Nanjo, A. Sekiguchi, H. Sakurai, *Bull. Chem. Soc. Jpn.* **1998**, *71*, 741.
- [15] C. Kayser, R. Fischer, J. Baumgartner, C. Marschner, *Organometallics*, in press.
- [16] K. W. Klinkhammer, W. Schwarz, *Z. Anorg. Allg. Chem.* **1993**, *619*, 1777.
- [17] K. W. Klinkhammer, *Chem. Eur. J.* **1997**, *3*, 418.
- [18] H. Weiss, H. Oehme, *Z. Anorg. Allg. Chem.* **1989**, *572*, 186.
- [19] R. Fischer, C. Marschner, unpublished results.
- [20] A. C. Hopkinson, M. H. Lien, *Tetrahedron* **1981**, *46*, 998.
- [21] A. C. Hopkinson, M. H. Lien, *J. Org. Chem.* **1981**, *37*, 1105.
- [22] R. Damrauer, J. Hankin, *Chem. Rev.* **1995**, *95*, 1137.
- [23] A. A. Brinkmann, S. Berger, J. I. Brauman, *J. Am. Chem. Soc.* **1994**, *116*, 8304.
- [24] M. S. Gordon, D. E. Volk, D. R. Gano, *J. Am. Chem. Soc.* **1989**, *111*, 9273.
- [25] A. C. Hopkinson, M. H. Lien, *Int. J. Quant. Chem.* **1978**, *13*, 349.
- [26] C. C. Levin, *J. Am. Chem. Soc.* **1975**, *97*, 5649.
- [27] M. R. Nimlos, G. B. Ellison, *J. Am. Chem. Soc.* **1986**, *108*, 6522.
- [28] D. J. Hajdasz, R. R. Squires, *J. Am. Chem. Soc.* **1986**, *108*, 3139.
- [29] C. Yamada, E. Hirota, *Phys. Rev. Lett.* **1986**, *56*, 923.
- [30] J. C. Sheldon, J. H. Bowie, C. H. DePuy, R. Damrauer, *J. Am. Chem. Soc.* **1986**, *108*, 6794.
- [31] J. V. Ortiz, *J. Am. Chem. Soc.* **1987**, *109*, 5072.
- [32] G. W. Spitznagel, T. Clark, P. v. R. Schleyer, W. J. Hehre, *J. Comput. Chem.* **1987**, *8*, 1109.
- [33] M. Shen, Y. Xie, Y. Yamaguchi, H. F. Schaefer, III, *J. Chem. Phys.* **1991**, *94*, 8112.
- [34] M. Shen, H. F. Schaefer, III, *Mol. Phys.* **1992**, *76*, 467.
- [35] K. Aarset, A. Császár, E. L. Sibert, III, W. D. Allen, H. F. Schaefer, III, W. Klopper, J. Noga, *J. Chem. Phys.* **2000**, *112*, 4053.
- [36] P. v. R. Schleyer, T. Clark, *J. Chem. Soc. Chem. Commun.* **1986**, 1371.
- [37] T. Wu, X. Chen, J. Peng, C. Shen, G. Ju, Q. Ju, *Int. J. Quant. Chem.* **2000**, *79*, 17.
- [38] P. C. Gomez, M. Alcolea Palafox, L. F. Pacios, *J. Phys. Chem. A* **1999**, *103*, 8537.
- [39] L. F. Pacios, O. Galvez, P. C. Gomez, *J. Phys. Chem. A* **2000**, *104*, 7617.
- [40] H. Pritzkow, T. Lobreyer, W. Sundermeyer, N. J. R. van Eikema, P. von R. Schleyer, *Angew. Chem.* **1994**, *106*, 221; *Angew. Chem. Int. Ed.* **1994**, *33*, 216.
- [41] M. A. Ring, D. M. Ritter, *J. Phys. Chem.* **1961**, *65*, 182.
- [42] O. Mundt, G. Becker, H.-M. Hartmann, W. Schwarz, *Z. Anorg. Allg. Chem.* **1989**, *572*, 75.
- [43] a) M. J. Frisch, G. W. Trucks, H. B. Schlegel, G. E. Scuseria, M. A. Robb, J. R. Cheeseman, V. G. Zakrzewski, J. A. Montgomery, R. E. Startman, J. C. Burant, S. Dapprich, J. M. Millam, A. D. Daniels, K. N. Kudin, M. C. Strain, O. Farkas, J. Tomasi, V. Barone, M. Cossi, R. Cammi, B. Menucci, C. Pomelli, C. Adamo, S. Clifford, J. Ochterski, G. A. Petersson, P. Y. Ayala, Q. Cui, K. Morokuma, D. K. Malick, A. D. Rabuck, K. Raghavachari, J. B. Foresman, J. Cioslowski, J. V. Ortiz, B. B. Stefanov, G. Liu, A. Liashenko, P. Piskorz, O. Komaromi, R. Gomperts, R. L. Martin, D. J. Fox, T. Keith, M. A. Al-Laham, C. Y. Peng, A. Nanayakkara, C. Gonzalez, M. Challacombe, P. M. W. Gill, B. G. Johnson, W. Chen, M. W. Wong, J. L. Andres, M. Head-Gordon, E. S. Replogle, J. A. Pople, *Gaussian98, Revision A.7*, Gaussian, Inc., Pittsburgh, PA (USA), **1998**; b) C. Lee, W. Yang, R. G. Parr, *Phys. Rev. B* **1988**, *37*, 785; c) A. D. Becke, *J. Chem. Phys.* **1993**, *98*, 5648; d) E. D. Glendening, A. E. Reed, J. E. Carpenter, F. Weinhold, NBO Version 3.1.
- [44] A. St-Amant, D. R. Salahub, *Chem. Phys. Lett.* **1990**, *169*, 387.
- [45] D. R. Salahub, R. Fournier, P. Mlynarski, I. Papai, A. St-Amant, J. Ushio, *Density Functional Methods in Chemistry* (Eds.: J. Labanowski, J. Andzelm), Springer, New York, **1991**.
- [46] V. G. Malkin, O. L. Malkina, L. A. Eriksson, D. R. Salahub, *Theoretical and Computational Chemistry, Vol. 2* (Eds.: J. M. Seminario, P. Politzer), Elsevier, Amsterdam, **1995**, 273.
- [47] J. P. Perdew, Y. Wang, *Phys. Rev. B* **1992**, *169*, 387.
- [48] W. Kutzelnigg, U. Fleischer, M. Schindler, *NMR Basic Principles and Progress Vol. 23*, Springer, Berlin, **1990**.
- [49] E. Buncel, *Carbanions: Mechanistic and Isotopic Aspects*, Elsevier, Amsterdam, **1975**.
- [50] E. Buncel, B. C. Menon, *Comprehensive Carbanion Chemistry, Part A* (Eds.: E. Buncel, T. Durst), Elsevier, Amsterdam, **1980**.
- [51] C. M. Earborn, P. Hitchcock, K. Izod, A. J. Jaggar, J. D. Smith, *Organometallics* **1994**, *13*, 753.
- [52] P. B. Hitchcock, M. F. Lappert, W.-P. Leung, L. Diansheng, T. Shun, *J. Chem. Soc. Chem. Commun.* **1993**, 1386.
- [53] M. Flock, C. Marschner, unpublished results.
- [54] E. Magnusson, *Tetrahedron* **1984**, *40*, 2945.
- [55] J. R. Damewood, C. M. Haddad, *J. Phys. Chem.* **1988**, *92*, 33.
- [56] H. Marsmann, *NMR Basic Principles and Progress, Vol. 1* (Eds.: P. Diehl, R. K. E. Fluck), Springer, Berlin, **1981**, p. 65.
- [57] T. Heine, A. Goursot, G. Seifert, J. Weber, *J. Phys. Chem. A* **2001**, *105*, 620.
- [58] A. Dransfeld, P. von R. Schleyer, *Magn. Reson. Chem.* **1998**, *36*, 29.
- [59] J. A. Tossell, P. Lazzeretti, *Chem. Phys. Letters* **1986**, *132*, 464.
- [60] G. Gutkunst, A. G. Brook, *J. Organomet. Chem.* **1967**, *9*, 67.
- [61] G. A. Olah, R. J. Hunadi, *J. Am. Chem. Soc.* **1980**, *102*, 6989.

Received: August 3, 2001 [F3465]